FAULT ANALYSIS OF DOUBLY FED INDUCTION GENERATOR BASED WIND TURBINE USING CROWBAR

This thesis is submitted in the partial fulfilment of the requirements of the degree

MASTER IN ELECTRICAL ENGINEERING

Submitted by

Suman Kundu

Examination Roll Number: **M4ELE22004**

Registration Number: **153994** of **2020–2021**

Under the Guidance of

Dr. Debashis Chatterjee

and

Mr.Nikhil Mondal

and

Mr.Mihir Hembram

Department of Electrical Engineering

Jadavpur University

Kolkata–700032

June, 2022

Faculty Council of Engineering and Technology

Jadavpur University

Kolkata- 700032

Certificate

This is to certify that the thesis entitled "Fault Analysis of Doubly fed Induction generator-based Wind Turbine using Crowbar", submitted by Suman Kundu (examination Roll No:- M4ELE22004), under the supervision and guidance of Dr.Debashis Chatterjee, Professor, Electrical Engineering Department, Jadavpur University, Mr.Nikhil Mondal,Associate professor, Electrical Engineering Department, Jadavpur University and Mr.Mihir Hembram,Assistant Professor, Electrical Engineering Department, Jadavpur University. We are satisfied with his work, which is being presented for the partial fulfilment of the degree of Master in Electrical Engineering from Jadavpur University, Kolkata-700032.

Dr.Debashis Chatterjee
Professor
Electrical Engineering Department
Jadavpur University
Kolkata-700032

Prof. Saswati Mazumdar
Head of the department
Electrical Engineering Department
Jadavpur University
Kolkata-700032

Mr. Mihir Hembram
Assistant Professor
Electrical Engineering Department
Jadavpur University
Kolkata-700032

Prof.Chandan Mazumdar
Dean
Faculty Council of Engineering and Technology
Jadavpur University
Kolkata-700032

Mr. Nikhil Mondal
Associate Professor
Electrical Engineering Department
Jadavpur University
Kolkata-700032

Faculty Council of Engineering and Technology

Jadavpur University

Kolkata-700032

Certificate of Approval

This is to certify that the thesis entitled “Fault Analysis of Doubly fed Induction generator-based Wind Turbine using Crowbar”, presented by Suman Kundu (Examination Roll No. M4ELE22004, Registration No. 153994 of 2020-21) to Jadavpur University for the partial fulfilment of the Degree of Master in Electrical Engineering, is hereby approved by the committee of final examination and that the student has successfully defended the thesis in the viva-voce examination.

Final examination for evalution of thesis

Signature of Examiners

_____

_____

Declaration of Originality

I declare that this thesis is an original report of my research, has been written by me and has not been submitted for any previous degree. The experimental work is almost entirely my own work; the collaborative contributions have been indicated clearly and acknowledged. Due references have been provided on all supporting literatures and resources**.**

Name : SUMAN KUNDU

Examination Roll No. : M4ELE22004

Thesis Title : Fault Analysis of Doubly fed Induction generator-based Wind turbine using Crowbar.

Signature with Date :

ACKNOWLEDGEMENTS

I express my sincere gratitude to my supervisor Dr.Debashis Chatterjee, Mr.Nikhil Mondal, Mr.Mihir Hembram for their encouragement, suggestion and advices, without which it would not have been possible to complete my thesis successfully. I would like to thank colleague Mr.Subhranil Chakraborty for being a constant source of encouragement, inspiration and for his valuable suggestions coupled with his technical expertise throughout my research work. It was a great honour for me to pursue my research under his supervision.

I would also like to express my gratitude to my friend Mr.Chandan Mahato and Mr.Tapas Sadhukhan for their support and guidance through the completion of the thesis. I have learnt a lot from their in the field of power doubly fed induction generator, AC to DC converter, DC to AC converter.

Last but not the least I extend my words of gratitude to my parents for personally motivating me to carry out the work smoothly.

Suman Kundu
Jadavpur University
Kolkata-700032

CONTENTS **PAGE No.**

ABSTRACT

This thesis focuses on the single line to ground fault of the Doubly Fed Induction Generator (DFIG). The Conventional PI controller with Crowbar protection scheme is applied to the DFIG for the control of the torque, the dc link voltage, rotor speed and the fault current. The grid connected DFIG is simulated and with the controller blocks for the rotor side converter and grid side converter control.

The Crowbar protection scheme of the DFIG is performed by applying stator and rotor flux orientation control scheme in synchronously rotating dq frame for the stator side. The DFIG based Wind Energy Conversion System system due to variable speed application and low converter rating makes it one of the most popular wind turbines used. The variable speed application of theDFIG is conducted in this thesis. The Crowbar protection scheme is one of the most popular control scheme. The current loops and the overall Crowbar protection scheme are studied in detail in the thesis. The maximum power point tracker is also implemented to maximize the power output of the wind turbine generator system. Furthermore, the analysis of the crowbar protection system to protect the system under unsymmetrical voltage dips is also performed.

LIST OF ACRONYMS

P_m = Mechanical Power Generated by Wind Turbine.

P_s = Stator Active Power of Doubly Fed Induction Generator.

V = Wind Speed.

A = Blade Swept Area.

ρ = Air Density.

P_r = Rotor Active Power of Doubly Fed induction Generator

Q_s = Stator Reactive Power of Doubly Fed Induction Generator

Q_r = Rotor Reactive Power of Doubly Fed Induction Generator

T_m = Mechanical Torque generated by wind turbine

ω_s = Rotational speed of synchronously rotating frame

ω_r = Rotating Speed of Rotor

R_s = Stator Resistance

R_r = Rotor Resistance

L_s = Stator Inductance

L_r = Rotor Inductance

L_m = Mutual Inductance

i_{ds}, i_{qs} = Direct and quadrature axis current of Stator

i_{dr}, i_{qr} = Direct and quadrature axis current of Rotor

V_{ds}, V_{qs} = Direct and quadrature axis voltage of Stator

V_{dr}, V_{qr} = Direct and quadrature axis voltage of Rotor

T_{em} = Electromagnetic Torque generated by the system

J = Moment of Inertia of wind turbine

LIST OF FIGURES

LIST OF TABLES

CHAPTER 1

INTRODUCTION

1.1. Introduction to Wind Energy Conversion System (WECS):

Wind energy conversion systems (WECS) are used to convert the energy of wind movement into mechanical power with wind turbine generators, this mechanical energy is converted into electricity and in windmills this energy is used to do various work . In the past, the power in the wind was utilized to provide useful mechanical power but in modern world WECS is mainly concentrated on conversion of energy to electrical form. The conversion of the wind energy into the electrical energy depends on several factors like angle of attack, tower height, wind speed, blade length, turbine type,etc[1].

Various types of conditions and equations are there to construct wind turbine generator . 1) Output power of a wind generator is proportional to the area swept by the rotor that means double the swept area and the power output will also double. 2) The power output of a wind generator is proportional to the cube of the wind speed. Kinetic Energy = $(1/2)mV^2$, where m = mass of air (in kg), V = velocity of air (in m/s), and the energy is given in joules[2]. Air has a known density (around 1.23 kg/m3 at sea level), so the mass of air hitting our wind turbine (which sweeps a known area) each second is given by the following equation: Mass/sec (kg/s) = Velocity (m/s) x Area (m2) x Density (kg/m3). Therefore, the power (i.e. energy per second) in the wind hitting a wind turbine with a certain swept area is given by simply inserting the mass per second calculation into the standard kinetic energy equation given above resulting in the following vital equation: $P = 0.5A\rho C_p V^3$.Where, P= Power in Watts, A= Swept area in square metres, ρ = Air density in kilograms per cubic metre, and V =Velocity of air in m/sec[3].

1.2. Introduction to Doubly fed Induction Generator:

A Doubly Fed Induction generator is a 3 phase induction generator where both the rotor and stator windings are fed with 3 phase AC signal. It consists of three phase windings placed on both the rotor and stator bodies. It also consists of a multiphase slip ring assembly to transfer power to the rotor. It is generally used to generate electricity in wind turbine generators.

Doubly Fed Induction Generators are widely used in Wind energy conversion system. This type of generators are basically a type of induction generator, where the Stator side is connected to the grid (Utility grid or microgrid) directly, whereas the rotor is also connected to the grid with the help of a back to back converter, where in between the rectifier and inverter side, there is a DC link capacitor which provides the reactive power. This type of configuration is helpful for smooth control of active power and reactive power.

.

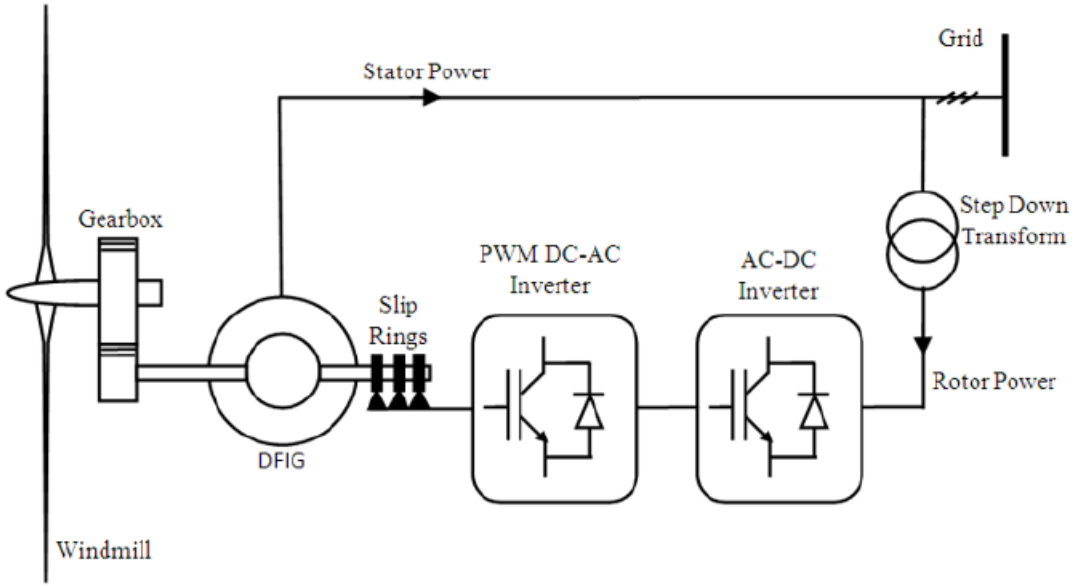

Figure 1.1: Block diagram of a typical wind turbine connected doubly fed induction generator

The figure 1.1 represents the block diagram of a typical wind turbine connected Doubly fed induction generator. The wind turbine is connected to the doubly fed induction generators with the help of a gearbox. As previously mentioned, the stator is connected with the grid

side and the rotor is connected to the grid with the help of a back-to-back converter. The dc link capacitor is located between the two converters. The chopper is used for overvoltage protection during voltage dip, the crowbar circuit is connected across rotor which is used to protect the whole circuit against surge current caused by sudden drop of the grid voltage during the fault period.

1.2.1.Working Principal of DFIG:

The DFIG consists of a 3 phase wound rotor and a 3 phase wound stator. The rotor is fed with a 3 phase AC signal which induces an ac current in the rotor windings. As the wind turbines rotate, they exert mechanical force on the rotor, causing it to rotate. As the rotor rotates the magnetic field produced due to the ac current also rotates at a speed proportional to the frequency of the ac signal applied to the rotor windings. As a result a constantly rotating magnetic flux passes through the stator windings which cause induction of ac current in the stator winding. Thus the speed of rotation of the stator magnetic field depends on the rotor speed as well as the frequency of the ac current fed to the rotor windings**.**In a DFIG based system a three-winding transformer gives different voltage levels for stator and rotor side. When the machine produces energy, only a small part of the generated power flows from the rotor to the grid. The converters can then be chosen in accordance with this small rotor power. This means smaller converters compared to fully rated converters and this allows to decrease the costs. The stator windings are connected to the grid which imposes the stator current frequency The stator currents create a rotating magnetic field in the air gap. The rotational speed of this field ω_s , s, is proportional to f_s.

$$\omega_s = 2\pi f_s \tag{1}$$

If the rotor spins at a speed different from that of the rotational field, it sees a variation of magnetic flux. Therefore, by Faraday's law of induction, currents are induced in the rotor windings . The DFIG machine operates usually as a generator if $\omega_r > \omega_s$ and as a motor otherwise. In the case of the DFIG however, it can operate in sub-synchronous mode as a generator. The slip, s, defines the relative speed of the rotor compared with that of the

$$S = \frac{\omega_s - \omega_r}{\omega_s} \quad (2)$$

The slip is usually negative for a generator and positive for a motor. The currents induced in the rotor windings pulse at an angular speed defined by the difference between the synchronous speed and the rotor speed. Indeed, the stator currents at ω_r sees the rotating magnetic field created by the stator pulsating at $\omega_s - \omega_r$.It means the frequency of the rotor currents,

$$f_r = sf_s \quad (3)$$

If the rotor were to rotate at the synchronous speed, it would not see any change in magnetic fluxes. No currents would then be induced in its windings. Therefore, the machine operates always at speeds different from synchronous speed. The rotor-side inverter controls the rotor currents. From equation (3), it can be noted that controlling the rotor currents controls the slip and so the speed of the machine.

1.3. Work Objective:

Different types of fault can occur in Doubly fed Induction generator when it is connected to the wind turbine. From Power system point of view, two types of faults are there, 1. Open Circuit fault, 2. Short Circuit fault. Again, if we classify Short circuit fault, then they are 2 types, 1. Symmetrical Fault, 2. Unsymmetrical Fault . And Unsymmetrical faults are also three types ,a) Single line to ground fault b) Line to line fault c) Double line to ground fault.

This paper concentrates on the low voltage ride-through capability of doubly fed induction generator (DFIG) wind turbines during and after the single lie to ground fault. The main attention in the paper is, therefore, drawn to the control of the DFIG wind turbine and of its power converter and to the ability to protect itself without disconnection during grid faults. The paper provides also an overview on the interaction between variable-speed DFIG wind turbines and the power system subjected to disturbances, such as short circuit faults. A typical grid code is displayed in the following figure 1.2.

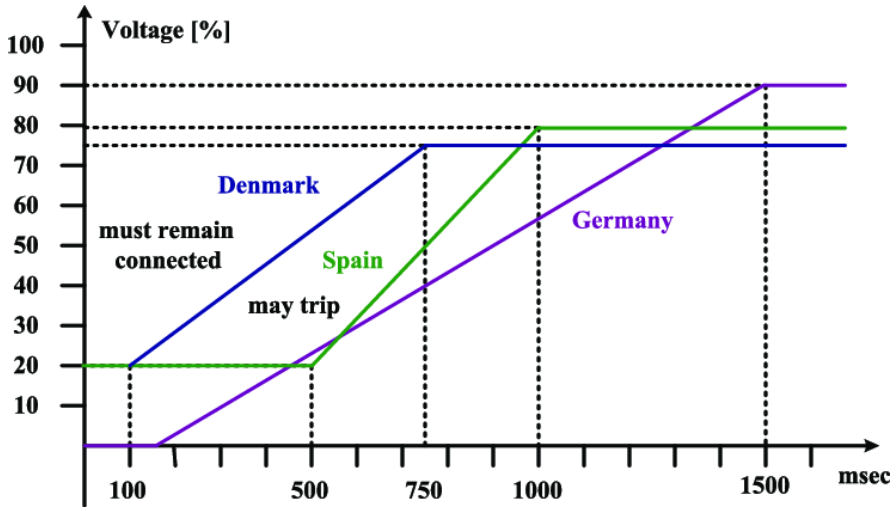

Figure 1.2: Grid codes in different countries for fault ride through

1.4. Thesis Organization:

The structure of this dissertation reflects the research objectives discussed above. Chapter two reviews existing FRT approaches and illustrates their performance. The third chapter of the thesis presents the introduction to conventional PI controller with crowbar protection approach of the doubly fed induction generator. Also, the relevant theory and the equations from the aerodynamics tothe electrical modelling of the system is presented in fourth chapter. This chapter also presents the vector control scheme for the induction generator, the current loops and the tuning of the PI controllers..The fifth chapters deal with the simulation and validation of the result. The wind turbine performance is observed. It demonstrates the results from Matlab/Simulink and discussion.The sixth chapter of the thesis concludes the research. It also points out the future works on the system.

Chapter 2
Literature Review

2.1. Introduction:

Electrical Energy is the most essential part in our social and economic growth . Non-renewable source of energy is creating a global concern. On the other hand source of fossil fuel is limited that is why the interest in the renewable energy sources is increasing day by day. The wind energy is one the most favorable best solution for the energy concern over the non-renewable sources.

In this chapter, we will discuss about different Fault ride through techniques that have been applied in previous work. In chapter 1, it is presented that the fault ride through technique in DFIG based wind turbine can be employed by 2 methods, 1. Auxiliary hardware-based method, 2. Software Based control technique. As this particular work is a combination of both hardware and software-based fault effect mitigation technique, I have mentioned the pre-existing works of the both techniques in the subsequent sections. Among these, some works have employed only Hardware based technique, some papers have employed software-based technique, and some papers have undertaken hybrid technique for fault mitigation.

2.2 Techniques employed for LVRT in DFIG :

Fault ride through techniques are basically two types , a) Auxiliary hardware based method, b) Software based method.

Where “Auxiliary hardware based method” is five types such as-

i) Crowbar approach.

ii) Fault current limiter.

iii) Static synchronous compensator

iv) Nine switch based approach.

v) Fault current limiter.

And ‘Software based method’ ia also five types such as-

i) Conventional PI control.

ii) Virtual damping flux based method.

iii) Inductance emulating control method.

iv) Feedforward current reference control approach.

v) Sliding mode approach.

2.2.1 Crowbar :

In this method , the fault characteristic and its formation mechanism of double-fed induction generator (DFIG) are explained, from the point of view of power system crowbar protection. A new method of analyzing and calculating fault current of DFIG is presented, which combines the advantages of physical process analysis and frequency domain analysis. According to the physical process analysis, the frequency domain equation of DFIG is divided into several equations about zero state and zero input response. By separately solving the several equations, formulas for calculation of the fault current are deduced. These formulas are not only applicable to calculation of short circuit current under symmetrical fault but also unsymmetrical fault. Based on this method, the fault current characteristics of DFIG under symmetrical and unsymmetrical fault are compared. Comparison result shows that AC component of fault current of DFIG under symmetrical fault soon decays end. But AC component under unsymmetrical fault is stable at the end. These new characteristics have an effect on the applicability of the traditional relay protection, and provide a theoretical basis for new methods of relay protection. At the end, simulation results show validity of the proposed formulas under symmetrical and unsymmetrical fault.

2.2.2. Fault current limiter :

This is used to limit the stator currents, that protects the doubly-fed induction generator wind turbine (DFIG-WT) during the symmetrical and asymmetrical grid faults. Fault current limiter is cost-effective and requires little maintenance during operation. They maintain rotor current and DC-link voltage below the maximum acceptable limits, thus, fortify the back-back converters. Similar to a crowbar circuit, the fault current limiter circuitry also consists of diode bridge circuitry. In paper [20], [21] different works related to fault current limiter are presented.

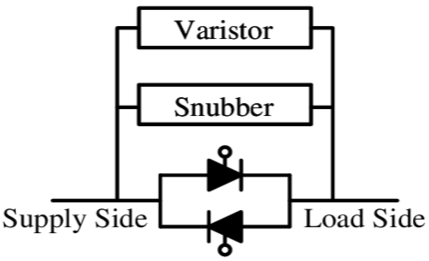

Figure 2.1) Resistive fault current limiter

2.2.3. Static Synchronous Compensator(STATCOM):

By controlling the amount of reactive power STATCOM regulates the terminal voltage of DFIG. When terminal voltage is low then the STATCOM generates reactive power and when terminal voltage is high then the STATCOM absorbs rective power from the line. A STATCOM is a capacitor based shunt-connected FACTSs device that is capable of generating and/or absorbing reactive power. Usually, the STATCOM is applied to voltage support aims. Recently, a large number of wind turbines installed are the variable speed type fitted with DFIGs. Under normal operating conditions, the DFIGs operate at close to unity power factor and may supply some reactive power during system disturbances such as a three-phase fault close to the wind farm in order to meet the LVRT grid code requirements. In fault period, when voltage of the grid becomes very low, The STATCOM then activates and fed reactive power to the system in order to prevent the voltage collapse. In this paper [18], the STATCOM based LVRT approach is undertaken with the help of gate turn-off thyristor (GTO) PWM converter with a dc-link capacitor.

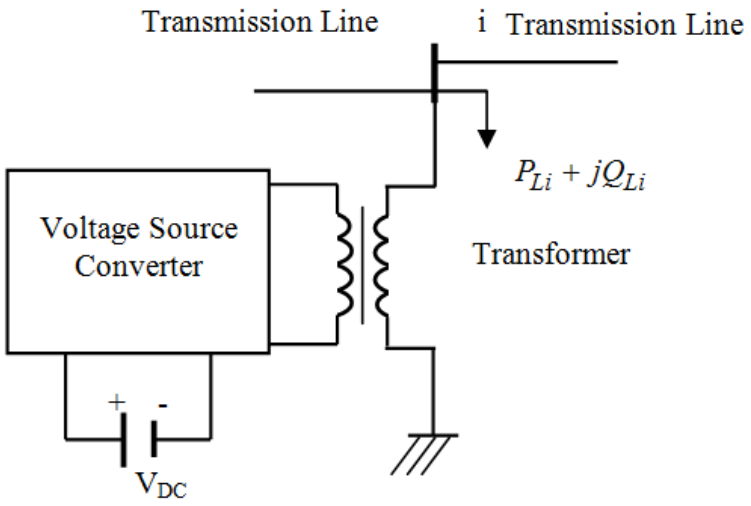

Figure 2.2) STATCOM regulator

2.2.4. Nine Switch Converter based DFIG :

In this case novel Nine-Switch Converter is used instead of the twelve-switch back-to-back converter. Its main features are sinusoidal output, unity power factor It costs reduced due to less number of switches.

It is the replacement of traditional twelve-switch back-to-back (B2B) converter [11]. With the proposed control, the gird-side branch gets higher voltage to maintain dc bus steady under normal condition, and the rotor-side branch gets higher voltage to withstand the rotor-overvoltage during Low Voltage Ride Through (LVRT). The proposed system and adapted control method ensure the rating capacity of the power devices can be fully used at any time, and no extra capacity margin on the power devices is required. Considering a traditional twelve-switch B2B converter requires extra capacity margins on its power devices, or additional auxiliary circuit to realize LVRT, the proposed NSC based system is more cost-efficient because it not only saves three power devices, but also achieves LVRT without additional auxiliary circuit. In most applications, thehigh dc voltage is the major defect of a NSC, which limits its application. In the DFIG wind power system, this high dc voltage could be properly utilized to withstand the rotor-overvoltage during the voltage dipping moment, and thus, achieves the LVRT without any additional auxiliary circuits. The advantages of NSC hardwares in DFIG wind power system, is that it only requires nine power switches so they are cost effective and dc voltage can be fully utilisedin either normal or LVRT period, and no extra voltage margin is required. [19]

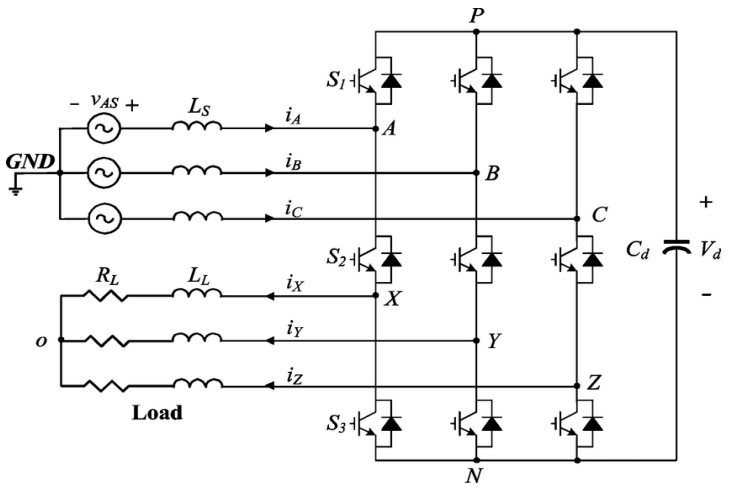

Figure 2.3) Topology of nine switch converte

2.2.5. Dynamic voltage restorer:

The working principle of Dynamic voltage restorer is almost similar to the series grid side converter.It is used to inject required magnitude of voltage and frequency so that DFIG can maintain actual voltage across the load end during low voltage ride ride through[3]. The aim of DVR system is to inject the voltage to produce the desired stator voltage. So, the stator terminal is kept nominal voltage continuously under both normal and grid fault conditions including balanced and unbalanced voltage dips[4]. For effective control of the DVR, digital all-pass filters are used for extracting the positive-sequence component from the unbalanced grid voltage since they have the advantages of giving a desired phase shift and no magnitude reduction over conventional low or high-pass filters. Using the positive-sequence component, the phase angles for the positive and negative sequence components of the grid voltage are derived. A control algorithm for the DVR that is dual voltage controllers only is implemented for the two sequence components in the *dq* synchronous reference frame. In order to achieve the power rating reduction of the DVR, the stator power reference for the DFIG is reduced during faults. In addition, a control scheme of pitch angle system is applied to stabilize the operation of the wind turbine system in the event of grid faults.

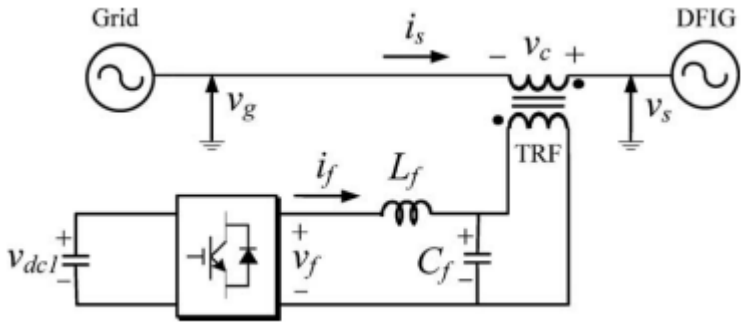

Figure 2.4. Dynamic voltage restorer

2.3. Software based Approach:

This technique is mainly software-based control techniques, where different types of mathematical manipulations are done, in order to improve the performance. This includes virtual damping flux based method, Impedance emulating method, PI control approach method etc[5].

These solutions are to improve the control strategy of RSC to fulfil the LVRT requirement. A robust controller is used in to improve the system transient response. Virtual impedance is introduced in some papers to increase the system damping. Since these two methods still use the same rotor current references of the conventional vector control method, i.e., the rotor current only contains the positive-sequence component, RSC should output sufficiently high voltage to offset EMF. However, such required rotor voltage cannot be outputted under severe 8 grid faults, because EMF far exceeds the RSC's maximum output voltage. In this case, the control system is prone to losing its controllability.

Some examples of software-based approaches are:

2.3.1. Conventional PI controller-based approach:

It is the most primitive process of controlling a grid side and rotor side converter. In fact, there is nothing special in this method because the presence of this type of controller is inevitable in DFIG based wind turbines. They generally are associated with crowbars, in order to protect the rotor windings from overcurrent or other hardware devices.

2.3.2 Virtual Damping flux based approach:

During the fault condition, the transient flux causes an huge overshoot in rotor current. To suppress that, a virtual damping flux based approach is undertaken . In this method, we virtually calculate the amount of flux and then apply it in a separate loop to diminish the effect of it.

2.3.3. Feedforward Current Reference Approach:

However, the classical proportional-integral (PI) controller cannot provide precise control of the transient and negative-sequence rotor current, because such current references in synchronous reference frame (SRF) are AC components at grid frequency and double grid frequency, respectively. To solve this problem, this paper proposes a feedforward current references control (FCRC) method for rotor side converter (RSC) to improve the system transient control performance.

2.3.4. Inductance Emulating Control:

For doubly fed induction generator (DFIG)-based wind turbines, the rotor side of DFIG is prone to suffering from overcurrent during grid faults, due to large electromotive force (EMF) induced in the rotor circuit. To solve this problem, this paper proposes an inductance-emulating control strategy for DFIG-based wind turbine to suppress the post-fault rotor current, thereby enhancing its low-voltage ride through (LVRT) capability. Under the proposed control strategy, once the grid fault is detected, the rotor side converter (RSC) is controlled to emulate an inductance[7].

2.3.5. Sliding Mode Control based approach:

Sliding mode control is a nonlinear robust control methodology by which anerror-based sliding surface is chosen. The objective of sliding mode control is to minimize the error between the reference and measured value to bring sliding surface=0 in finite time. Sliding surfaces are to be chosen such a way that Lyapunov criteria is satisfied. In paper [7], the DFIG grid fault has been minimized with the help of a sliding mode control-based methodology.

Chapter 3

Introduction to Conventional PI controller with Crowbar protection Approach

3.1. Introduction:

In chapter 2, we already put some views over Crowbar protection scheme and conventional PI controller approach. Now for this particular thesis work, we have to introduce a newer type of , that is Conventional PI controller with Crowbar protection scheme . As we know, a typical Conventional PI controller based approach has several disadvantages, like high stator and rotor fault current phenomena, So in order to overcome this, we are using a different approach, Conventional PI controller with Crowbar protection scheme .It can be said as a part of conventional PI control, where a terminal attractor in mathematical form is used in order to alleviate the large overshoot and weak anti-disturbing phenomenon and to ensure the finite time convergence. In subsequent slides and in next chapter, we shall discuss about Conventional PI controller with Crowbar in more detail[9],[10].

3.2. Details of Conventional PI control:

The PI control is still the mostly used method within DFIG power system controls. Despite the merits of simple structure, easy realization and wide using range, this method has to be based on a precise model. When the controlled systems change their parameters or operating situations, the PI controllers' performance will decrease significantly. Considering the DFIG system is actually multiple parameters nonlinear system with complex dynamic parts, the traditional PI control can bring several defects, such as poor dynamic performance, large overshoot and weak anti-disturbing ability. For the problems of conventional PI controller we need to develop a system which can reduce the drawbacks[13],[14].

3.2.1. Mathematical Approach of Conventional PI Control:

To implement PI based control of DFIG machine, vector control approach is widely accepted and extended one. The vector control of the induction machine is understood by the current control loops. The vector control is an attractive solution for high performance and limited speed range drive system application . The use of the suitable power converter in the rotor

side, the overall system control can be performed with low current harmonic distortion in both stator and rotor side . The space vector theory is used to express the three-phase quantities in terms of the space vectors. Vector control modelling describes induction machine describes its transient and steady state performance. The three phase quantities are converted to synchronously rotating frame in order to address the system dynamics in aconvenient way. The system becomes simpler and simplifies the understanding of the control process. In the work, we specifically use stator flux-oriented vector control. In order to easily control the production of electricity by the wind energy conversion system the stator flux vector is aligned with d-axis. That results is-

$$\lambda_{ds}=\lambda_s \text{ and } \lambda_{qs}=0 \qquad (5)$$

Stator d and q axis voltage equations are-

$$V_{ds} = R_s I_{ds} + \frac{d\lambda_{ds}}{dt} - \omega_s \lambda_{qs} \qquad (6)$$

$$V_{qs} = R_s I_{qs} + \frac{d\lambda_{qs}}{dt} + \omega_s \lambda_{ds} \qquad (7)$$

Now by putting eqation-(5) value into the equation (6) and the equation (7) we get-

$$V_{ds} = R_s I_{ds} + \frac{d\lambda_{ds}}{dt} \qquad (8)$$

$$V_{qs} = R_s I_{qs} + \omega_s \lambda_s \qquad (9)$$

Rotor d and q axis voltages are -

$$V_{dr} = R_r I_{dr} + \frac{d\lambda_{dr}}{dt} - (\omega_s - \omega_r)\lambda_{dr} \qquad (8)$$

$$V_{qr} = R_r I_{qr} + \frac{d\lambda_{qr}}{dt} - (\omega_s - \omega_r)\lambda_{qr} \qquad (9)$$

Similarly, the fluxes in the stator and the rotor can be represented in the stationary reference frame as follows:

$$\lambda_{ds} = L_s I_{ds} + L_m I_{dr} \qquad (10)$$

$$\lambda_{qs} = L_s I_{qs} + L_m I_{qs} \qquad (11)$$

$$\lambda_{dr} = L_r I_{dr} + L_m I_{ds} \qquad (12)$$

$$\lambda qr = L_r I_{qr} + L_m I_{qs} \qquad (13)$$

Assuming λ_{ds} to be constant in steady state, Suppose that electrical supply network is stable, which leads to constant stator flux which means derivative term of λ_{ds} is also zero.So the new voltage equation will be:

$$V_{ds} = RsI_{ds} \qquad (14)$$

$$V_{qs} = R_s I_{qs} + \omega_s \lambda_s \qquad (15)$$

3.2.2 Decoupled control of active and reactive power :

Variable speed wind energy system uses mostly doubly-fed induction generators(DFIGs) for its application which gives better performance, maximum power output etc. Various control scheme is used for both machine-side converter control and grid-side converter control. stator-flux oriented vector control scheme is used in machine-side converter by which decouple control of active and reactive of DFIG is achieved. Grid voltage oriented vector control is used in grid-side, which maintains the dc-link voltage and improves the power factor at rotror-side.The function of the rotor side (RSC) is to control the active and reactive powers of DFIG. Since the DFIG is connected to the utility grid, the power produced by the generator must be controlled independently . Hence, the stator flux oriented vector control is introduced for this reason, which consists to align the stator flux vector position along *d*-axis, as shown in figure below.

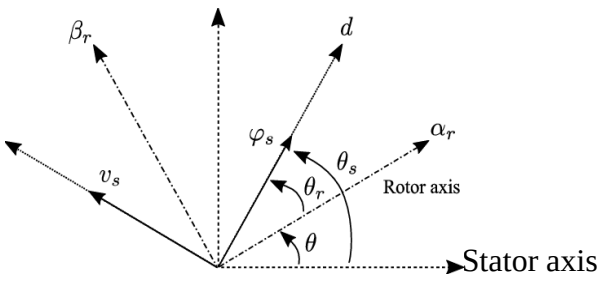

Figure 3.1. Stator and rotor flux vectors of DFIG

3.2.3) Details of Crowbar protection circuit :

For DFIG (Doubly Fed Induction Generator) based wind turbines, crowbar is a commonly used protection method against surge current caused by sudden drop of the grid voltage during the period of LVRT (Low Voltage Ride-Through). Based on detailed analysis of the transient flux characteristics of DFIG with the crowbar fired, a simplified model is proposed to analyze and approximate the short circuit current accurately. Meanwhile the maximum short circuit current and the LVRT capability are evaluated. After that the dc-link voltage clamp effect is pointed out and a crowbar design method based on the dc-link voltage is proposed accordingly.

A Crowbar Circuit is a simple electrical circuit that prevents damage to the circuits (load of the power supply) in the event of an overvoltage of the power supply. It protects the load by shorting the output terminals of the power supply when a overvoltage is detected.When the output terminals of the power supply are shorted, the huge current flow will blow the fuse and thus disconnecting the power supply from the rest of the circuit. Hence, in simple terms, the job of the Crowbar Circuit is to detect the overvoltage ,overcurrent and blow the fuse (sometimes, a circuit breaker is tripped).Typically, Crowbar Circuits are designed using Thyristor (SCR).

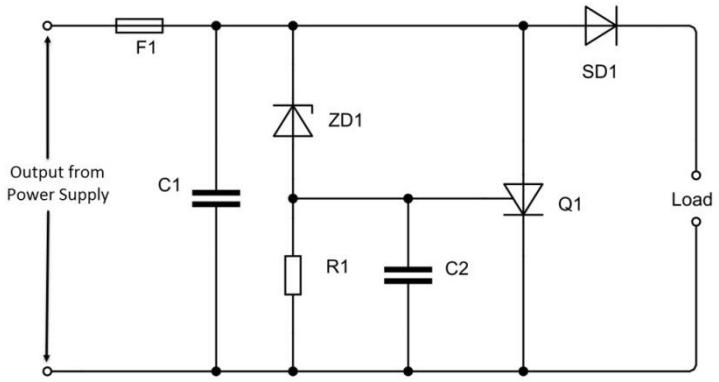

Figure 3.2. Crowbar circuit by using SCR

3.2.4 Working principle of Crowbar :

The working of Crowbar circuit is very simple. The Zener Diode (ZD1) is the component that detects the over voltage. Usually, the threshold voltage of the Zener Diode is selected just over the output voltage of the power supply (1V more than the output voltage).

When an overvoltage occurs and if the voltage reaches the threshold voltage of the Zener Diode, then it starts conducting. If the voltage still increases, the voltage drop across the Resistor R1 and the Gate terminal of the SCR (Q1) will increase.

Initially, when the Zener Diode in not conducting, the Resistor R1 acts as pull-down resistor for the Gate terminal of the Thyristor to keep in LOW. But when the Zener Diode starts conducting and the voltage across the resistor R1 increases, the gate voltage also increases.

When the voltage at the Gate terminal is more than its threshold voltage (usually between 0.6V and 1V), the Thyristor starts to conduct and essentially providing a short circuit between the power rails. As a result of this short circuit, the fuse blows.One important point to remember here is that the current rating of the Thyristor should be more that that of the Fuse. Also, the overall trigger voltage is the sum of Zener Diode threshold voltage and the Thyristor threshold voltage.There are few other components in the circuit and let us see their purpose in this circuit. First, the Capacitor C1 is a filter capacitor used to reduce noise and small voltage spikes and avoids unnecessary triggering of the circuits. The Capacitor C2 is a Snubber Capacitor and it prevents accidental triggering of the Thyristor during powerup of the circuits. Finally, the Schottky Diode acts as reverse protection diode to prevent the main circuit from triggering the Crowbar Circuit.

3.4. Chapter Summary:

In this chapter, the theoretical approaches that are to be undertaken for the thesis work has been discussed. The conventional PI controller and Conventional PI controller with Crowbar protection scheme have been presented efficiently**.**

Chapter 4
Mathematical Formulation For Test Simulation

4.1. Introduction:

In this chapter we shall discuss about mathematical formulation that is required for our simulation. As discussed in chapter 3, we shall start with the mathematical modelling of DFIG. This will give us the set of equations that we can use to create our Conventional PI controller with Crowbar scheme.

4.2. Mathematical modelling of Wind turbine:

Wind turbine converts the kinetic energy present in the wind to the mechanical energy. The generated mechanical energy is in the form of torque and speed [14]. The mechanical power produced has the cubic power relation with the wind velocity so fluctuations in the wind speed creates the variation in the generated power. The total energy present in the wind is given by:

$$P_m = \frac{1}{2}\rho A V_w^3 \qquad (16)$$

The mechanical power and the torque of the wind turbine is given by:

$$P_m = \frac{1}{2}\rho\pi R^2 V_w^3 C_p \qquad (17)$$

$$T_t = \frac{1}{2}\rho\pi R^3 V_w^2 C_t \qquad (18)$$

Where,

ρ = Density of the air = 1.23 Kg/m3

A = π R^2 = Cross sectional area of the blade.

R= Radius of the wind turbine.

Cp=Power coefficient.

Ct= Torque Coefficient = Cp/λ

λ = Tip Speed Ratio =$\frac{R\ \Omega t}{V_w}$

In the above equation the power and the torque coefficients are used since only the fraction of the total kinetic energy present in the wind is converted into the mechanical energy at the wind turbin. The power conversion coefficient is the function of the blade pitch angle (β) and the tip to speed ratio (λ). The tip to speed ratio is the speed of the tip of the turbine blade relative to the speed of the wind. The generated power depends on the relative velocity of the rotor tip and the wind speed.

The extracted power from the wind turbine can be controlled by controlling the Cp value. During the higher winds, the generator and the converter can be overloaded. At these conditions the rotor speed must be controlled. This is done by rotating the pitch of the blade. The graph below shows the relationship between the power conversion coefficient and tip to speed ratio for different values of the pitch angle.

4.3. Mathematical modelling of DFIG :

The mathematical modelling of DFIG is based on dq axis modelling. Making it into rotating reference frame, it is easier to analyse the system. DFIG is currently the most widely used types of electrical generators for wind turbine systems in the Megawatt range .

A synchronous rotating dq reference frame is used to model the DFIG with the direct -axis oriented along the stator flux position. In this way, decoupled control between the electrical torque and the rotor excitation current is obtained. The reference frame is rotating with the same speed as the stator voltage[20],[21]. The schematic diagram of the grid connected DFIG is shown in figure 1.1.

4.3.1. dq to abc convertion:-

The Clarke transformation transforms the 3-phase system a,b,c to the two orthogonal coordinate system (α,β). This transformation transforms the three phase reference frame to the two-phase stationary reference frame [15].

The Park Transformation transforms the 3 phase a,b,c co-ordinate into a synchronously rotating dq0 reference frame. To perform this, one more parameter is needed which is the angular position ωt, unit in radian. When the rotating frame alignment at ωt=0 is 90 degrees behind the phase A axis, a positive-sequence signal with Mag=1 and Phase=0 degrees yields the following dq values: d=1, q=0.[16]

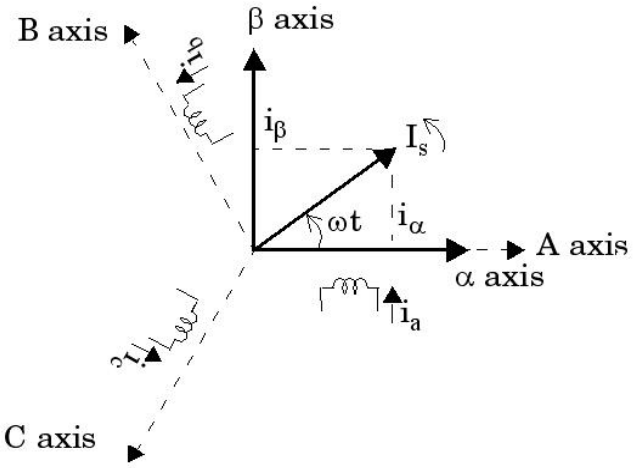

Figure 4.1. dq to abc conversion model

4.3.2 Rotor side converter :

The vector control of the machine is performed in the synchronously rotating *dq* reference frame. The stator flux vector position is oriented along the direct-axis[23],[24]. The implementation of the control of the rotor side converter the stator and rotor currents along with the stator voltage and rotor position is required to be known. The advantage of the stator flux orientation is that the torque is only dependent on the quadrature axis component of the rotor current. The equations obtained for the rotor voltage in synchronous reference frame as the function of the rotor currents is as shown in figure 4.2 -

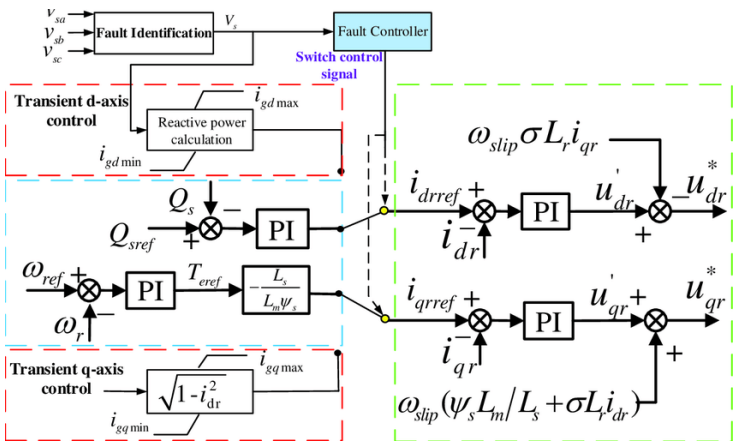

Figure 4.2. Controller of rotor side converter

4.3.3. Equivalent dq axis circuit of DFIG:

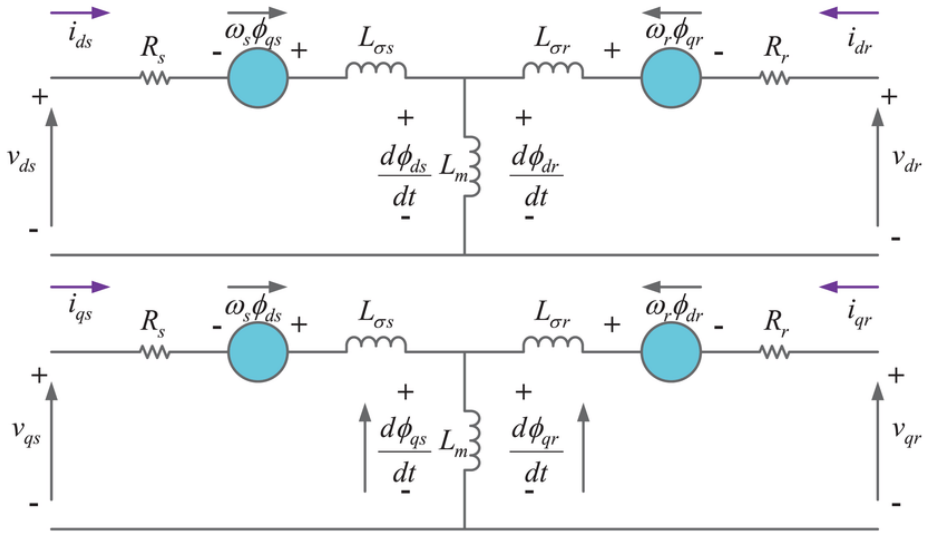

Figure 4.3. d-q model of DFIG

From the figure, the voltage equations can be derived as follows:

$$V_{ds} = R_s I_{ds} + \frac{d\lambda_{ds}}{dt} - w_s \lambda_{qs} \qquad (19)$$

$$V_{qs} = R_s I_{qs} + \frac{d\lambda_{qs}}{dt} + w_s \lambda_{ds} \qquad (20)$$

$$V_{dr} = R_r I_{dr} + \frac{d\lambda_{dr}}{dt} - (w_s - w_r)\lambda_{dr} \qquad (21)$$

$$V_{qr} = R_r I_{qr} + \frac{d\lambda_{qr}}{dt} - (w_s - w_r)\lambda_{qr} \qquad (22)$$

Change of d-q frame current will be-

$$\frac{dI_{qr}}{dt} = \frac{1}{\sigma L_r}\left(V_{qr} - R_r I_{dr} - sV_{qr}\,\sigma I_{dr} - \frac{s\omega_s L_m \lambda_s}{L_s}\right) \qquad (23)$$

And $$\frac{dI_{dr}}{dt} = \frac{1}{\sigma L_r}\left(V_{qr} - R_r I_{qr} + sV_{dr}\sigma I_{qr}\right) \quad (24)$$

The fluxes in the stator can be written as follows:

$$\psi_{ds} = L_s i_{ds} + L_m i_{dr} \quad (25)$$

$$\psi_{qr} = L_s i_{qs} + L_m i_{qr} \quad (26)$$

Similarly, for the fluxes in the rotor can be written as:

$$\psi_{dr} = L_m i_{ds} + L_r i_{dr} \quad (27)$$

$$\psi_{qr} = L_m i_{qs} + L_r i_q \quad (28)$$

Where, *Ls Lr and Lm* are the stator, rotor and the mutual inductances respectively.Also,

$$L_s = L_{\sigma s} + L_m \quad (29)$$

$$L_r = L_{\sigma r} + L_m \quad (30)$$

Where $L_{\sigma s}$ and $L_{\sigma r}$ are the self-inductances of the stator and the rotor respectively.

4.3.4. Back to back PWM converter:

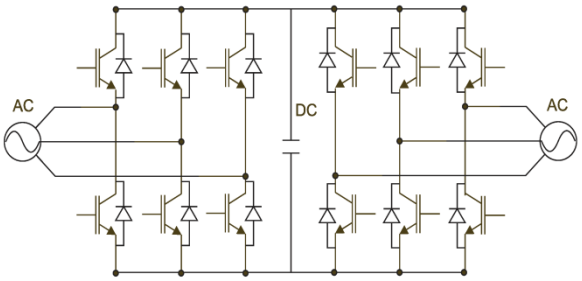

Figure: 4.4. Schematic of Back to Back PWM converter

Power circuit of three-phase voltage-source back-to-back PWM converters including twelve power semiconductor switches is shown in Fig.4.4, where the two converters are linked through a DC capacitor. As can be seen in Fig. 4.4, the AC/DC converter has three input voltages and produces an output voltage (DC voltage), which is the input voltage of the

inverter, whereas the three phase voltages designate the output terminal of the inverter.RSC and GSC can be considered as two controllable voltage sources. These two voltage sources can be expressed in a reference frame where the stator voltage space vector is aligned with the *q*-axis. Note that the reference frames for DFIG model, RSC control, and GSC control are all aligned with the stator voltage[25].

The RSC and GSC voltages are generated through the afore-mentioned control blocks. In Matlab/Simulink, feedback control blocks can be built. The converter controls can then be integrated with the DFIG model in the same *dq* reference frame.There is one relationship not modelled yet: the DC-link capacitor dynamics or the relationship between the RSC and the GSC. The DC-link capacitor dynamics has to be considered as well[26].

4.3.5 Grid side converter :-

The control objective of the grid side converter is to keep the DC-link voltage constant regardless of the magnitude and the direction of the rotor power. Direct axis current is controlled to keep the DC-link voltage constant, and quadrature axis current component can be used to regulate the reactive power flow between the grid side converter and the grid. The d-axis of the reference frame is aligned with the grid voltage angular position. Since amplitude voltage of the grid is constant, Vqg is zero and Vdg is constant[27],[28].

The active and reactive powers injected to the grid by the Converter can be calculated as follows:

Active Power, $P_{dg} = 3/2\ (V_{dg}I_{df} + V_{qg}I_{qf})$ (31)

Or, $P_{dg} = 1.5V_{dg}I_{df}$ (32)

Reactive Power,

$Qg = 3/2(V_{qg}I_{df} - V_{dg}I_{qf})$ (33)

Or, $Qg = -1.5V_{dg}I_{qf}$ (34)

In a typical grid filter model, the voltage equation can be written as follows:

$V_{df} = R_fI_{df} + Lf$ (35)

where V_{df}, V_{qf} are the voltages at the output of GSC and Idf, Iqf are the corresponding reactive power flow between the supply side converter and the supply will be proportional to idf and iqf respectively. The amount of energy stored in the DC-link capacitor is given by:

$dw/dt = ½\ C\frac{d^2V}{dt} = -P_f - Pr$ (36)

And, equivalent d-q axis voltage is given by-

$$V_{dg}^{eq} = (\frac{2}{3}\frac{\sigma}{V_{dg}} L_f P s_{ref} + \mathrm{RfI_{df}} + \omega_s \mathrm{L_f I_{qf}} - \mathrm{V_{dg}}) \quad (37)$$

And,

$$V_{qf}^{eq} = (-\frac{2}{3}\frac{\sigma}{V_{dg}} L_f Q s_{ref} + \mathrm{R_f I_{qf}} + \omega_s \mathrm{L_f I_{qf}}) \quad (38)$$

4.4. Conventional PI controller based approach:

4.4.1. Tuning of the regulators:

Rotor Side Converter Controller Tuning The equivalent block diagram for the closed loop current control in the rotor side control block is shown in the block diagram as below from

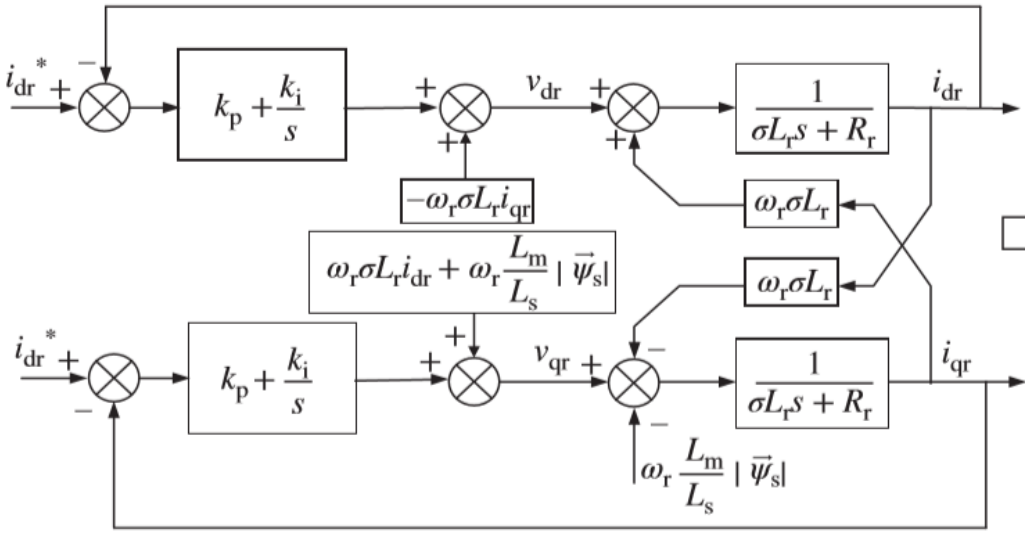

Figure 4.5. Current control loop of Rotor side converter with conventional PI control

The block diagram shown above can be simplified into the transfer function as below:

$$\frac{i_{dr}}{i_{dr}^*} = \frac{sK_p + K_i}{L_f s^2 \sigma + s(K_p + R_r) + K_i} \quad (39)$$

$$\frac{i_{dr}}{i_{qr}^*} = \frac{sK_p + K_i}{L_f s^2 \sigma + s(K_p + R_r) + K_i} \quad (40)$$

The above transfer function is then compared with the denominator of the second order of the general control transfer function i.e., $s^2 + 2\xi\omega_n s + (\omega_n)^2$
we have-

$$K_i = L_r(\omega_n)^2 + 2\,\sigma \qquad (41)$$

$$\text{And } Kp = 2\sigma L_r \xi(\omega n)^2 - R_r \qquad (42)$$

This gives the proportional and the integral gain constant for the PI-controller in the rotor side converter control.

4.4.2 Grid Side Converter Controller Tuning:

The grid side converter is fed from the grid using the RL-filter. Taking theLaplace transformation in the voltage equations of the grid side converter yields the following transfer function:

$$\frac{i_{dq}}{V_{df}} = \frac{1}{R_f + sL_f} \qquad (43)$$

$$\text{and } \frac{i_{qq}}{V_{qf}} = \frac{1}{R_f + sL_f} \qquad (44)$$

The block diagram for the grid side converter control loop is shown in the figure below**:**

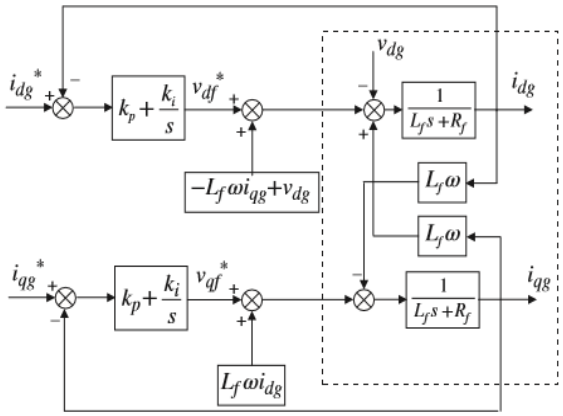

Figure 4.6. Current control loop of grid side converter with Conventional PI control

The current loops in the control block diagram can be modelled using the transfer function as shown below:

$$\frac{i_{dg}}{i_{dg}^*} = \frac{sK_p + K_i}{L_f s^2 + s(K_p + R_r) + K_i} \qquad (45)$$

$$\text{And } \frac{i_{qg}}{i_{qg}^{*}} = \frac{sK_p + K_i}{L_f s^2 + s(K_p + R_r) + K_i} \qquad (46)$$

This gives the proportional and the integral gain constant for the PI-controller in the rotor side converter control.

4.4.3 Design of the Control System for DFIG Wind Turbine in conventional PI controller:

The vector control of the induction machine is widely accepted and extended one. The vector control of the induction machine is understood by the current control loops. The vector control is an attractive solution for high performance and limited speed range drive system application [32], [33]. The use of the suitable power converter in the rotor side, theoverall system control can be performed with low current harmonic distortion in both stator and rotor side [23], [32]. The main idea behind the vector control of the induction machine is its mathematical equivalency to the separately magnetized dc machine [33]. The space vector theory is used to express the three-phase quantities in terms of the space vectors. This modelling of the induction motor describes the operation of the motor in the transient and the steady state[34]. The three phase electrical quantities are converted into two orthogonal components that can be visualized as the vectors. The projection converts the three-phase time dependent system to the two-component time invariant system. This helps us to visualize the three phase induction motor as that of the two-phase system[35]. The system becomes simpler and simplifies the understanding of the control process.

4.4.5 Rotor Side Converter:

The vector control of the machine is performed in the synchronously rotating *dq* reference frame. The stator flux vector position is oriented along the direct-axis [23], [36]. The implementation of the control of the rotor side converter the stator and rotor currents along with the stator voltage and rotor position is required to be known. The advantage of the stator flux orientation is that the torque is only dependent on the quadrature axis component of the rotor current The equations obtained for the rotor voltage in synchronous reference frame as the function of the rotor currents is as shown below:

$$V_{dr} = R_r I_{dr} + \frac{d\lambda}{dt} - (\omega_s - \omega_r)\boldsymbol{\lambda} \qquad (47)$$

And, $V_{qr} = R_r I_{qr} + \sigma L_r \frac{di_{qr}}{dt} - \sigma \omega_r L_r i_{dr} + \omega_r \frac{L_m}{L_s} \frac{d\psi}{dt}$ (48)

Where,

$$\sigma = 1 - \frac{L_m^2}{L_s L_r} \quad (49)$$

The stator flux is constant since the grid is connected to the stator of the DFIG, this implies that the derivative term $\frac{d\psi}{dt}$ is zero [31], [33]. For the transformation in the reference frame, the angle θ_r has to be estimated. The stator and the rotor winding turns ratio must be considered at the control stages of the induction machine. For the thesis, the rotor current i_{dr} is set to zero. The block diagram for the rotor side converter control of the induction machine is provided in figure 4.7.

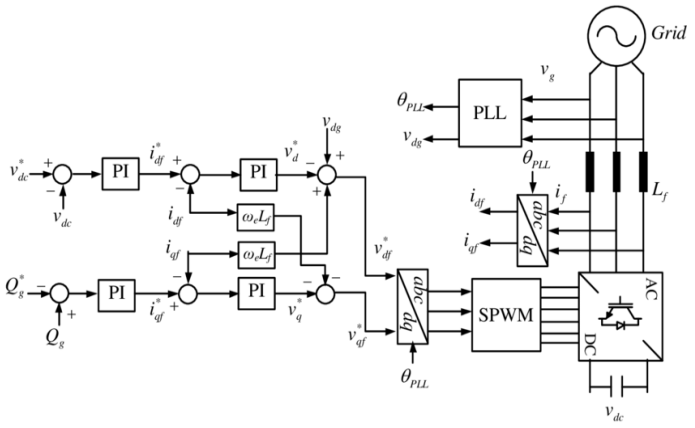

Figure 4.7. Block diagram for the rotor side converter control of the DFIG

In the block diagram, PLL(Phase Locked Loop) is used to estimate the grid angle while in this thesis the grid angle is calculated using angle calculation block which will explained in the later section.

And the controller constant gains in the above block diagram are defined as below-

$$K_{pg} = \frac{1}{\left(\frac{3}{2}\right)V_{dg}} \quad (50)$$

$$\text{and } K_{qg} = -\frac{1}{\left(\frac{3}{2}\right)V_{dg}} \quad (51)$$

4.4.6 Angle Estimation

For the estimation of the rotor angle and the grid angle an angle estimation block is used. The rotor angle can be calculated as follows:

$$\theta s = tan^{-1}\left(\frac{v_{s\alpha}}{v_{s\beta}}\right) \quad (52)$$

$$\text{And } \theta r = \theta s - \frac{\pi}{2} - \theta e \quad (53)$$

where,

$\theta e = p\theta m$

θs is the stator angle

θr is the rotor angle

θe is the electrical angle

Chapter 5

“ Simulation”

5.1 Model description:-

Matlab/Simulink model consists of wound induction generator, back toback PWM converters, Conventional In this chapter, the mathematical models of the Doubly Fed Induction Generator are realized using PI controller block, Crowbar and grid block. The measurement block is also present and the output block which consists of the scope from Matlab to view the results in the Simulink environment.The asynchronous wound induction generator from the Simscape library is used as the induction generator for the thesis[30],[31]. The stator of the generator is connected directly to grid while the rotor of the converter is connected to the back to back converter and to the grid.The IGBT based converters are used for the simulation purpose. One of the IGBT converteris connected to the rotor of the DFIG while the other converter is connected to the grid through the filter circuit. The DC link capacitor decouples the operation of the converters so that the individual control of the converter is made possible. The aerodynamics model generates the torque to drive the machine based on the formulas given in the previous chapters. The controller block consists of the rotor side controller and the grid side controller for the respective converters. The pulse signal to drive the converters are generated at the controller block [32].

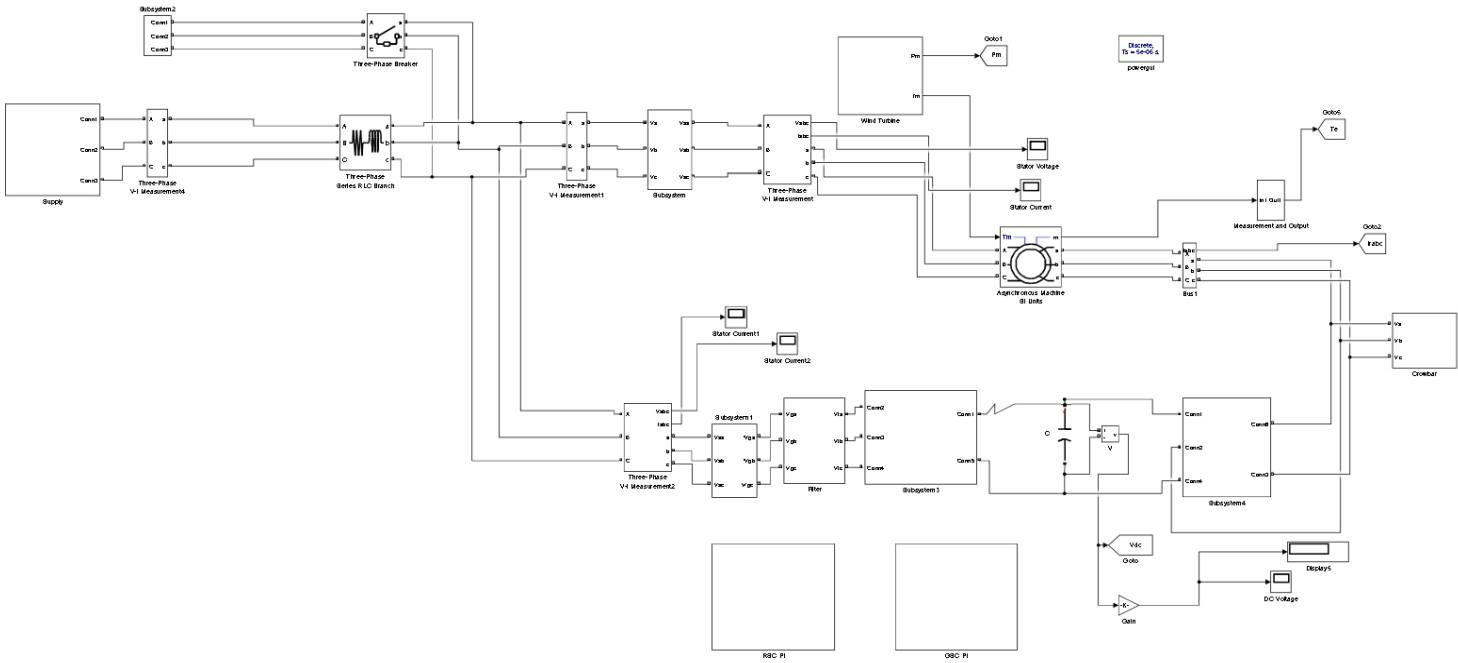

Figure 5.1. MATLAB/SIMULINK block diagram for simulation of unsymmetrical fault with conventional PI controller with crowbar.

The parameters used in the wound generator are summarized in the table below:

Table 5.1) Generator parameters

Parameters	**Values**
Number of pole Pairs	2
Stator Voltage	500
Rotor Voltage	500
Stator Resistance	0.0025
Stator Inductance	0.076 mH
Mutual Inductance	2.52 mH

Parameters	Values
Rotor Inductance	0.084 mH
Inertia	25
Friction Factor	0.025
Filter Resistance	0.19866 mohm
Filter Inductance	0.05262 mH
DC capacitor value	30000 μF
Crowbar Resistance	1 μohm

5.2.2. Controller blocks:

5.2.2.a. Rotor side controller :

The conventional PI control of the block diagram presented in the previous section is implemented in this section. The reference voltage for the rotor side converter is generated using the vector control. The block also consists of the Maximum Power Point Tracking block whichmaximizes the efficiency of the system by tracking the optimum operational speed. The block consists of the several transformation blocks which transforms the voltages and currents in the abc reference frame to the stationary reference frame and then to the synchronously rotating dq- reference frame. The PI controllers are used for the control. The gains of the PI controller are tuned which was explained in the previous section. The generated reference voltage is then fed to the PWM generator block from the Matlab/Simulink library. This block generates the pulse signal for the control of the rotor side converter. The figure below shows the Indirect Speed controller MPPT used in the control block[33],[34].

5.2.2.b. Grid Side Controller:

The grid side converter control discussed in the previous section is implemented in this section. The grid side converter (GSC) controls the dc-link voltage and regulates the reactive power exchange with the grid. The grid voltage orientation vector control is implemented[35],[36]. The control of the grid side converter requires the transformation of the abc-reference frame to the synchronously rotating dq reference frame. The grid side current inthe decoupled synchronous reference frame is controlled using the PI controllers. The PI controllers are tuned using the gain parameters derived in the previous section. The currentoutputs of the PI controller are then converted into the voltages converted back to the abc-reference frame. The signal is then applied to the PWM generator to generate the pulse signal for the grid side controller[37],[38].

5.3 Wind turbine Aerodynamics block:

The wind turbine block is made by utilising the equations of wind turbine as mentioned in chapter 4. The output of wind turbine is mechanical power and aerodynamic torque. The Torque is fed to the induction generator. The wind Turbine model uses wind speed, generator

speed and the pitch angle as the input parameters. The radius of the blade, and the wind speed is used to derive the power coefficient Cp(λ, β). Then, the torque calculated. The figure below shows the block which performs the aerodynamic calculation of the turbine torque[39],[40].

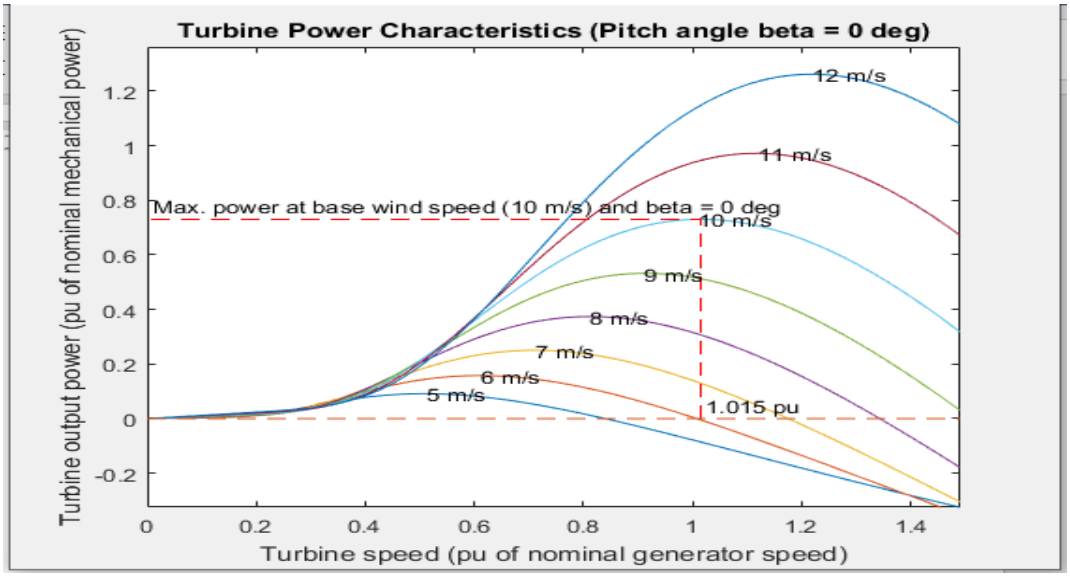

Figure 5.2. Wind turbine power characteristics

The optimum value of lambda is obtained from the Cp(λ, β) and tip to speed ratio curve. The optimum value of the power coefficient is the maximum value obtained from the curve and it is obtained to be 49% which is not practically viable. So, the value of Cp is chosen to be at 44%.[41],[42]. The rated parameters used in the aerodynamics block is shown below:

Table 5.2. Aerodynamic Properties:

Parameters	Values
Wind Speed	10 m/s.
Radius	35

Pitch Angle	0
Gear Box	80
Density of Wind	1.3

5.4 Simulation Test Scenario and Results :

Now we shall focus on our simulation work. To check the fault ride through capability with different types controllers, we have to introduce a fault in the grid side so that voltage dip occurs. Voltage dip is a sudden reduction of the voltage at a point in the electrical system between 10% and 100% and lasts for half cycle to 1 min[43],. Three-phase symmetrical faults represent one of the most common causes of voltage sags. In this work, we have introduced three phase symmetrical fault which results in a 100% dip of voltage in the DFIG grid side which implies that no grid voltage remains from 0.9 s to 1.1 s in the simulation runtime. A three-phase breaker is used purposefully to create the voltage dip on the aforementioned time interval. The simulation runtime is 2 second. The following figure represents the voltage waveform forthe time interval with fault condition.[44],[45]

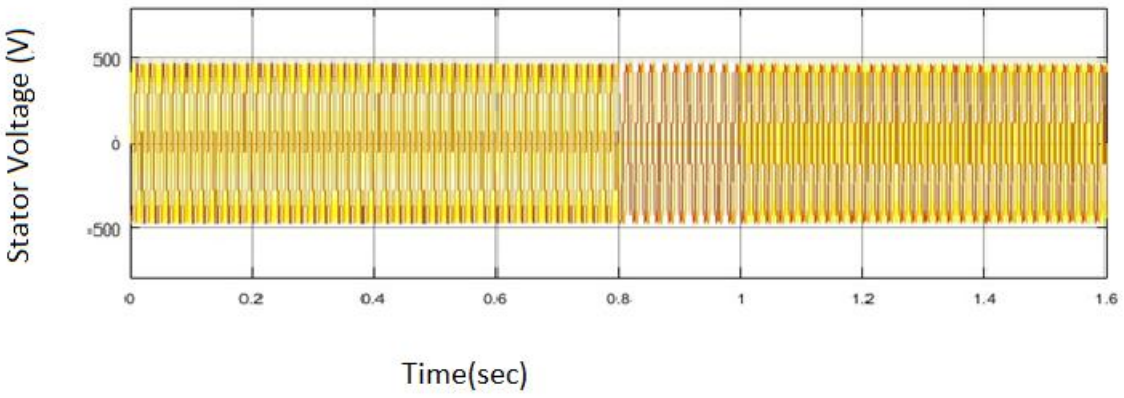

Figure 5.3) Grid voltage waveform without fault applied.

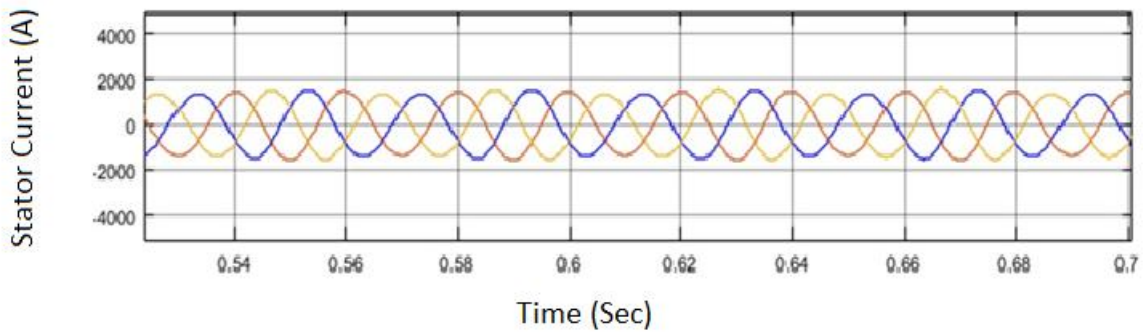

Figure 5.4. Normal waveform of stator current.

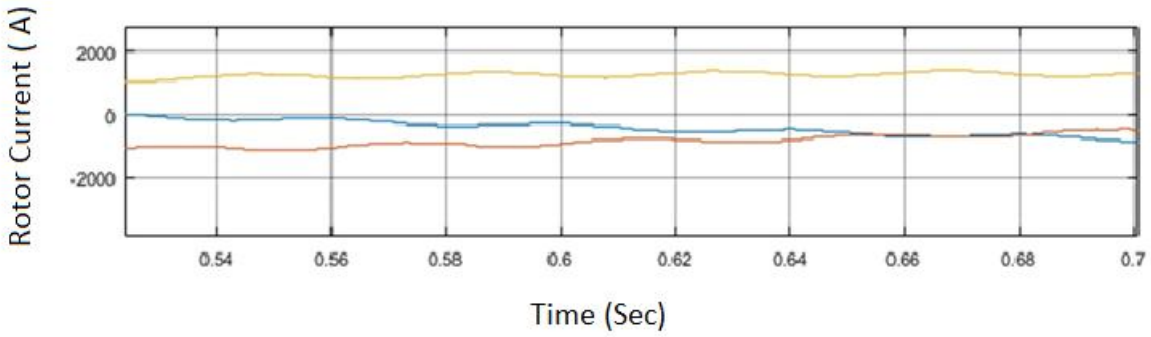

Figure 5.5. Normal waveform of rotor current

5.6 Unsymmetrical fault Using Conventional PI controller:

Now we have to check the effect on Stator voltage, stator current, rotor current ,torque ,active power and reactive power due to Unsymmetrical fault using conventional PI controller. This control approach implementation isdone in Rotor Side converter and grid side converter control block in the system model in SIMULINK. The mathematical implementation of the control is done as per the control methodology discussed in the chapter 4. Kp and Ki values for the controllers are calculated as per the equations derived[46],[47].

With this controller we have checked the response of Stator current, Rotor Current, Rotor Speed, Stator Active Power, Stator Reactive Power and Torque during the fault condition. From the graphs it can be seen that as soon as 0.8 sec time reached, the single line to ground fault initiates, resulting in a spike in stator and rotor current, and a fluctuation in torque, that eventually stabilizes at zero[48]. Active and Reactive Power becomes zero at fault time

because the Voltage is 0. Again after 1 sec, a huge transient occurs in stator and rotor current,a fluctuation occurs in active, reactive power and torque. This method offers poor control ineliminating harmonics from the system and yield poor output.

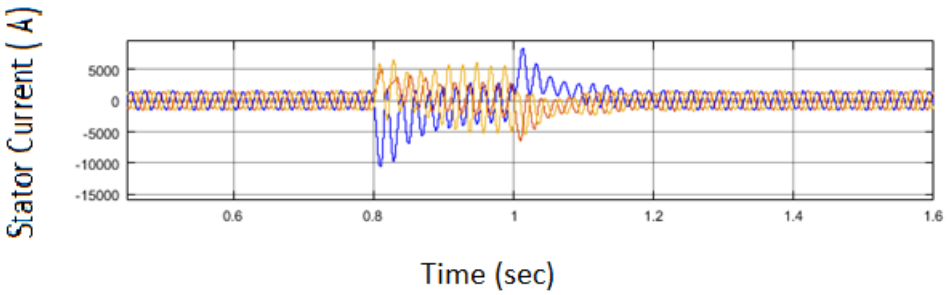

Figure 5.6.1. Stator current variation in conventional PI controller

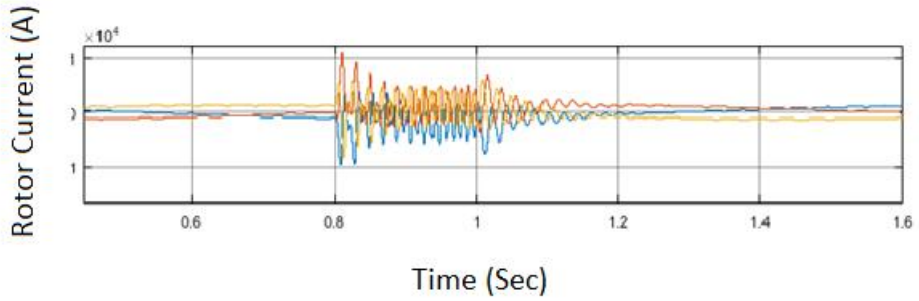

Figure 5.6.2. Rotor current variation in Conventional PI controller

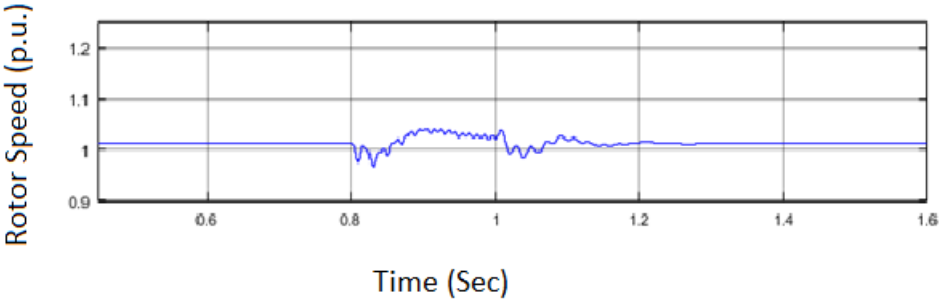

Figure 5.6.3. Rotor speed variation in Conventional PI controller

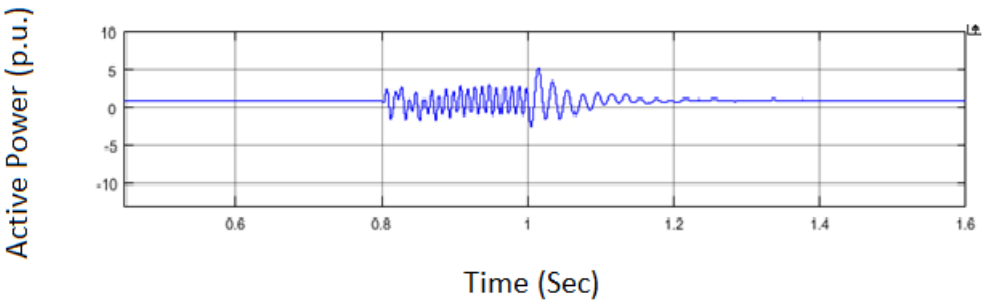

Figure 5.6.4. Active power variation in Conventional PI controller

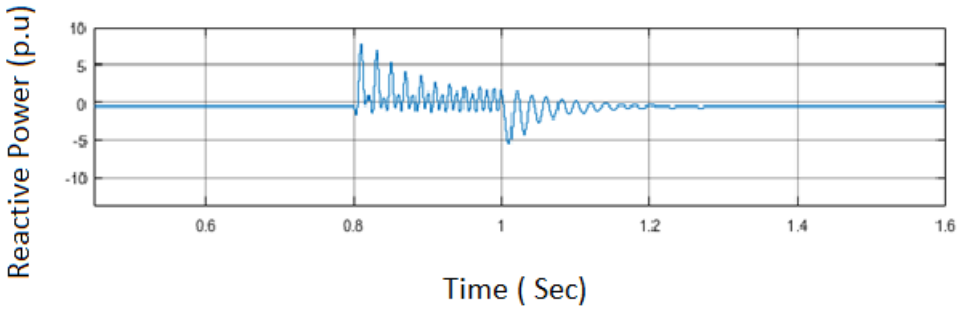

Figure 5.6.5. Reactive power variation in Conventional PI controller

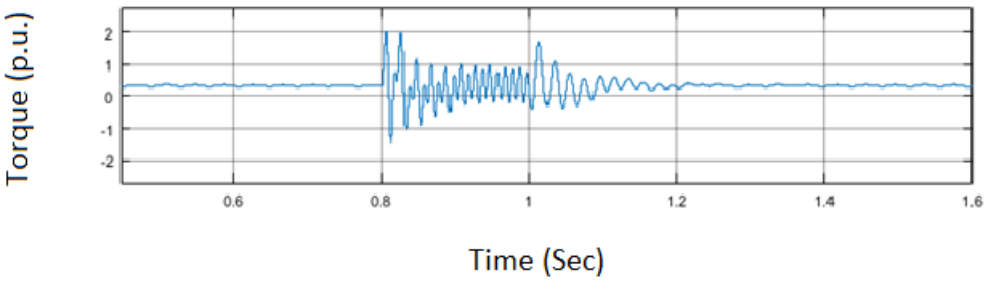

Figure 5.6.6. Torque variation in conventional PI controller

5.7 Unsymmetrical Fault analysis Using Conventional PI Controller with Crowbar protection :

Now we have to check the effect on Stator voltage, stator current, rotor current ,torque ,active power and reactive power due to Unsymmetrical fault using Conventional PI controller with crowbar protection scheme . This control approach implementation is done in Rotor Side converter and grid side converter control block in the system model in SIMULINK. The detailed mathematical expressions of Conventional PI controller with crowbar protection scheme is presented in chapter 3 and 4. Similar to PI controller, now we have to check the response of Stator current, Rotor Current, Rotor Speed, Stator Active Power, Stator Reactive Power and Torque during the fault condition. From the graphs it can be seen that as soon as 0.8 sec time reached, the single line to ground fault initiates, resulting in a spike in stator and rotor current, and a fluctuation in torque, that eventually stabilizes at zero. Active and Reactive Power becomes zero at fault time because the Voltage is 0. Again after 1 sec, a huge transient occurs in stator and rotor current, a fluctuation occurs in active, reactive power and torque. From the waveforms it can be concluded that the response is better than conventional PI controller in terms of generating better response.

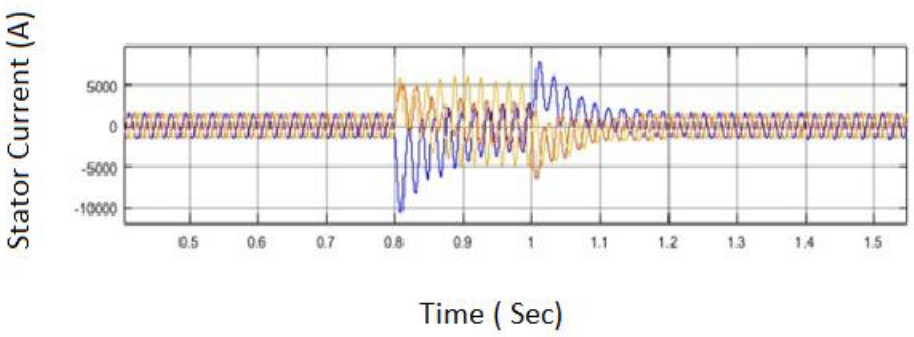

Figure 5.7.1. Stator current variation in “conventional PI controller with crowbar”

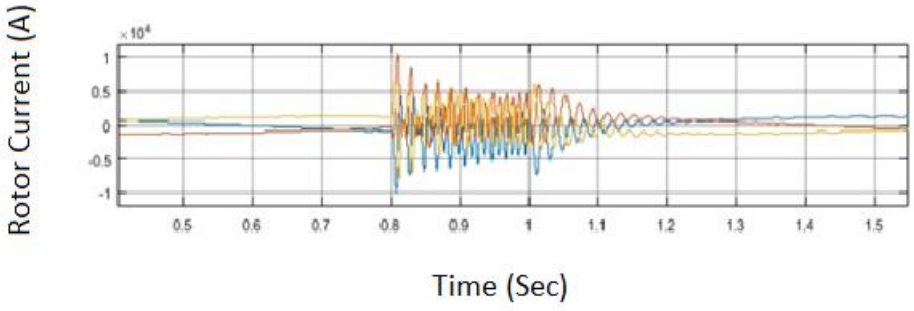

Figure 5.7.2. Rotor current variation in “conventional PI controller with crowbar”

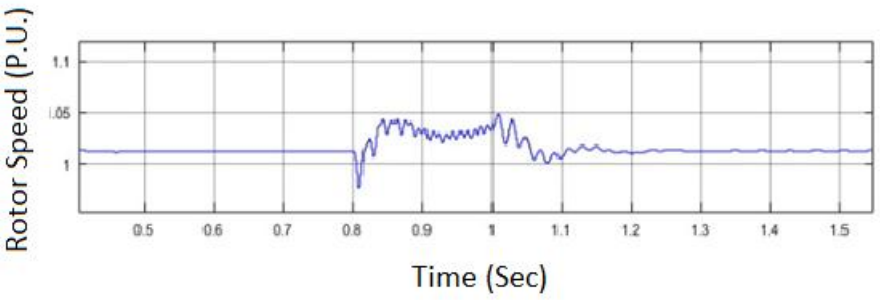

Figure 5.7.3. Rotor speed variation in "conventional PI controller with crowbar"

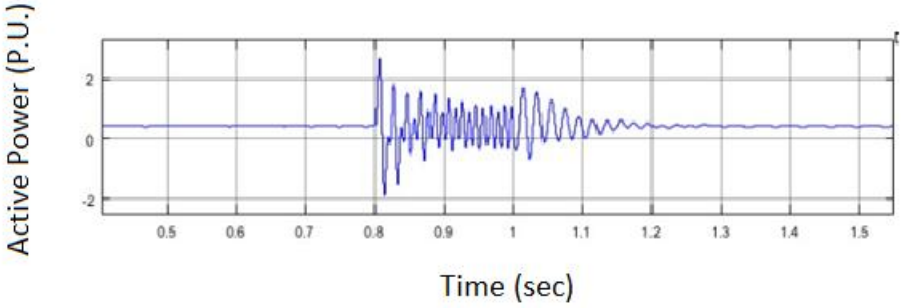

Figure 5.7.4. Active power variation in "conventional PI controller with crowbar"

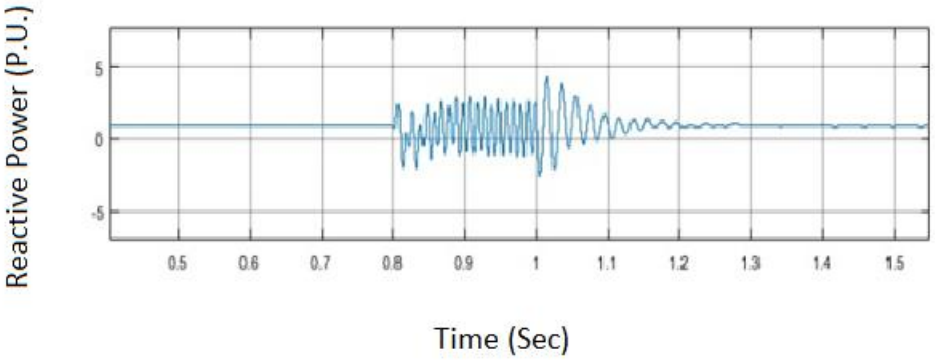

Figure 5.7.5. Reactive power variation in "conventional PI controller with crowbar"

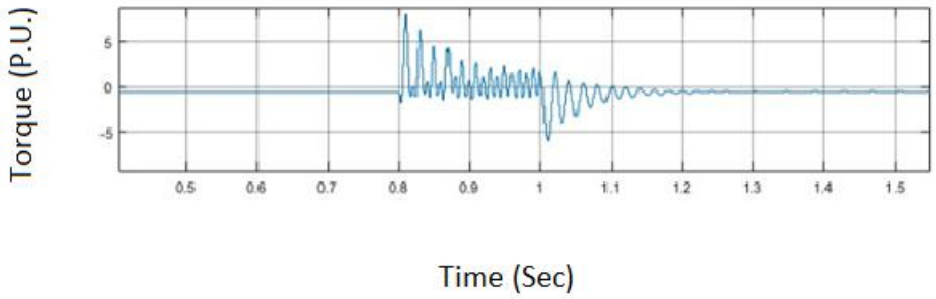

Figure 5.7.6. Torque variation in "conventional PI controller with crowbar"

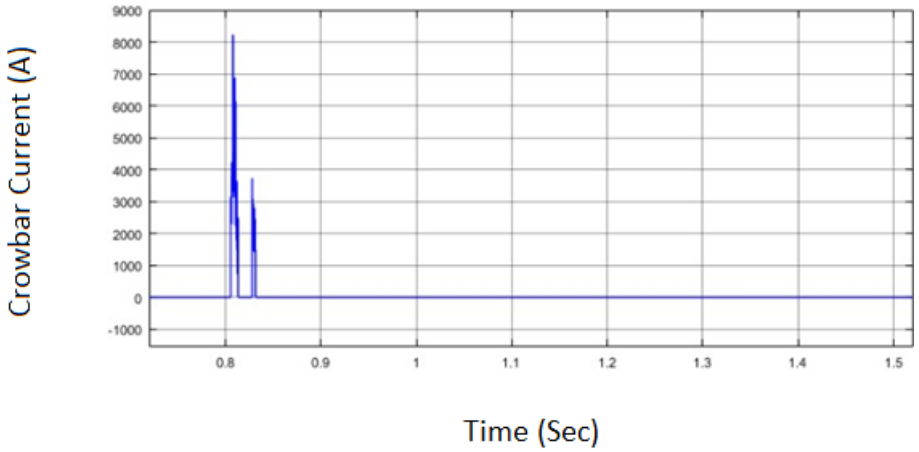

Figure 5.7.7. Crowbar current variation "conventional PI controller with crowbar"

Result summary :

From the obtained results, we can conclude that the proposed conventional PI controller with Crowbar protection scheme is much better in terms of eliminating high stator current,high rotor current, and improving torque variation , active power variation and reactive power control and it is also capable of ensuring finite time convergence as compared to conventional PI control . It is useful enough for the system to abide by the grid codes.

5.8. Data Comparison Table:

Different controllers	**Maximum Stator current in transient period (in pu)**	**Maximum Stator current in transient clearing time (in pu)**	**Settling time (in sec)**
PI controller	3.33	4.44	0.3
PI controller with Crowbar	2.77	3.88	0.25

5.4. Comparison of stator current transient characteristics

Different controllel	**Maximum rotor current in transient period (in pu)**	**Maximum rotor current in transient clearing time (in pu)**	**Settling time(in sec)**
PI controller	5.7	3.33	0.23
PI controller with Crowbar	5.55	2.77	0.2

5.5.Comparison of rotor current transient characteristics

Different controllels	**Stator active power in transient period (in pu)**	**Stator active power in transient clearing time (in pu)**	**Settling time(in sec)**
PI controller	0	5	0.3
PI controller with Crowbar	0	1.5	0.25

Table 5.6: Comparison of active power transient characteristics

Different controllel	**Stator reactive power in transient period(in pu)**	**Stator reactive power in transient clearing time(in pu)**	**Settling time(in pu)**
PI controller	0	5	0.4
PI controller with Crowbar	0	4	0.3

Table 5.7: Comparison of reactive power transient characteristics

Different controllel	**Torque in transient period(in pu)**	**Torque in transient clearing time(in pu)**	**Settling time(in sec)**
PI controller	2	1.5	> 0.4
PI controller with Crowbar	7	5	0.4

Table 5.8. Comparison of torque transient characteristics

Chapter 6
Conclusion and Future work

Conclusion :

In this thesis, Conventional PI controller with crowbar protection scheme is undertaken in order to enhance the fault characteristics and the fault ride through performance of DFIG based wind turbine. The objective of this thesis work is to improve the fault characteristics of DFIG due to single line to ground fault and improving the transient performance of the system. Single line to ground fault with 100% voltage sag is used in order to check the effect of L-G fault using the proposed scheme. The obtained results ensure the terminal attractor property of Conventional PI controller with crowbar protection scheme that alleviates the transient phenomenon in conventional PI control. Further, to reduce the current overshoot to some extent, we use a crowbar at rotor terminal and compare The compared result ensures the superiority of conventional PI control.

In this thesis, the vector control of the induction machine with stator flux orientation for the rotor side converter and the grid voltage orientation vector control for the grid side converter was performed. The thesis analyzes the operation of the DFIG on variable wind condition with maximum power point tracking. The successful control of the induction machine was achieved to generate the power. The operation of the DFIG in different operating speed was observed and the system was subjected to the variable wind speed.

The reference output signal was compared with the result of conventional PI controller scheme and conventional controller with crowbar protection scheme . The unsymmetrical voltage dip was analyzed, and the system was protected using the crowbar. Vector control of the DFIG is very important control technique that offers the dynamic control of the machine. The current loops are studied in detail. DFIG based WECS is oneof the important and most popular wind turbines. The low rating sizing of the converter and the variable speed application to be able to operate and control the turbine in subsynchronous and super-synchronous mode makes the DFIG scheme more popular.

Future Plans:

Wind energy is one of the most emerging field of energy. The more intensive and wide research on the renewable energy to reduce the environmental hazards caused by the fossil fuels. Variable speed wind energy is one of the most important renewable energy. But DFIG based Wind turbines are very prone to experience grid faults so, fault analysis is very important to maintain grid codes and to protect DFIG power converters from high rotor current. Lots of work were proposed in order to control grid fault in DFIG connected wind turbine. In this work our contribution is to present a crowbar protection scheme along with the conventional PI controller. This model can be further expanded to the stand-alone operation of the wind turbine with changes in the controller blocks. Also, This work further can be progressed by applying more robust control methodologies like H-infinity control, because the H-infinity control system has higher efficiency and adds more to the power system stability and security. The turbine model along with other sources can increase the stability as well as minimize the power system fluctuations.

References

[1] Z. Du and W. Gu, "Aerodynamics analysis of wind power," *WNWEC 2009 - 2009 World Non-Grid-Connected Wind Power Energy Conf.*, no. 1, pp. 235–237, 2009.

[2] H. S. Kim and D. D.-C. Lu, "Wind Energy Conversion System from Electrical Perspective—A Survey," *Smart Grid Renew. Energy*, vol. 01, no. 03, pp. 119–131, 2010.

[3] P. Pardalos, S. Rebennack, M. V. F. Pereira, N. A. Iliadis, and V. Pappu, *Handbook of Wind Power Systems*, vol. 3. 2014.

[4] X. Wang and Y. Shen, "Fault tolerant control of DFIG-based wind energy conversion system using augmented observer," *Energies*, vol. 12, no. 4, 2019.

[5] T. Ackermann and L. So, "An overview of wind energy-status 2002," vol. 6, pp. 67–128, 2002.

[6] T. Shanker and R. K. Singh, "Wind energy conversion system: A review," *2012 Students Conf. Eng. Syst. SCES 2012*, pp. 1–6, 2012.

[7] M. K. Johari, M. A. A. Jalil, M. Faizal, and M. Shariff, "Comparison of horizontal axis wind turbine (HAWT) and vertical axis wind turbine (VAWT)," no. October, 2018.

[8] G. Abad, J. López, M. A. Rodríguez, L. Marroyo, and G. Iwanski, *Doubly Fed Induction Machine*. 2011.

[9] T. M. Letcher, "Wind Energy Engineering-A Handbook for Onshore and Offshore Wind Turbines." .

[10] Å. K. E. Larsson, *The Power Quality of Wind Turbines Department of Electric Power Engineering*. 2000.

[11] P. Singh and A. Kaur, "Power control of doubly fed induction generator (DFIG) using back to back converters (PWM technique)," *Proc. 2014 IEEE Int. Conf. Adv. Commun. Control Comput. Technol. ICACCCT 2014*, no. 978, pp. 73–77, 2015.

[12] M. Cheng and Y. Zhu, "The state of the art of wind energy conversion systems and technologies: A review," *Energy Convers. Manag.*, vol. 88, pp. 332–347, 2014.

[13] L. H. Hansen, L. Helle, F. Blaabjerg, E. Ritchie, H. Bindner, and P. Sørensen, *Conceptual survey of Generators and Power Electronics for Wind Turbines*, vol. 1205, no. December. 2001.

[14] A. Perdana, *Dynamic Models of Wind Turbines*. 2008.

[15] Microsemi, "Park, Inverse Park And Clarke, Inverse Clarke Software, Transformations MSS Implementation," *Microsemi*, pp. 5–7, 2013.

[16] J. P. Lyons, S. M. Ieee, M. C. Robinson, P. Veers, and R. W. Thresher, "04596953,"

pp. 1–4, 2008.

[17] T. Ackermann and L. So, “Wind-energy-technology-and-current-status-a-review_2000_Renewable-and-Sustainable-Energy-Reviews,” vol. 4, 2000.

[18] G. M. Joselin Herbert, S. Iniyan, E. Sreevalsan, and S. Rajapandian, “A review of wind energy technologies,” *Renew. Sustain. Energy Rev.*, vol. 11, no. 6, pp. 1117–1145, 2007.

[19] X. Yingcheng and T. Nengling, “Review of contribution to frequency control through variable speed wind turbine,” *Renew. Energy*, vol. 36, no. 6, pp. 1671–1677, 2011.

[20] H. T. Jadhav and R. Roy, “A critical review on the grid integration issues of DFIG based wind farms,” *2011 10th Int. Conf. Environ. Electr. Eng. EEEIC.EU 2011 - Conf. Proc.*, pp. 1–4, 2011.

[21] S. Li, T. A. Haskew, and L. Xu, “DFIG characteristic and control integration study under decoupled d-q vector control in stator flux oriented frame,” *IET Conf. Publ.*, no. 538 CP, pp. 391–395, 2008.

[22] S. Muller, M. Deicke, and R. W. De Doncker, “Doubly Fed Induction Generator Systems,” *IEEE Indusry Appl.*, pp. 26–33, 2002.

[23] R. Pena, J. C. Clare, and G. M. Asher, “Doubly fed induction generator using back-to-back PWM converters and its application to variablespeed wind-energy generation,” *IEE Proc. Electr. Power Appl.*, vol. 143, no. 3, pp. 231–241, 1996.

[24] R. Pena, J. C. Clare, and G. M. Asher, “A doubly fed induction generator using back-to-back PWM converters supplying an isolated load from a variable speed wind turbine,” *IEE Proc. Electr. Power Appl.*, vol. 143, no. 5, pp. 380–387, 1996.

[25] E. B. Muhando, T. Senjyu, A. Uehara, T. Funabashi, and C. H. Kim, “LQG design for megawatt-class WECS with DFIG based on functional models’ fidelity prerequisites,” *IEEE Trans. Energy Convers.*, vol. 24, no. 4, pp. 893–904, 2009.

[26] M. F. Iacchetti, G. D. Marques, and R. Perini, “A scheme for the power control in a DFIG connected to a DC bus via a diode rectifier,” *IEEE Trans. Power Electron.*, vol. 30, no. 3, pp. 1286–1296, 2015.

[27] A. Dekhane, S. Lekhchine, T. Bahi, S. Ghoudelbourg, and H. Merabet, “DFIG modeling and control in a wind energy conversion system,” *2012 1st Int. Conf. Renew. Energies Veh. Technol. REVET 2012*, pp. 287–292, 2012.

[28] M. El Azzaoui, H. Mahmoudi, and K. Boudaraia, “Analysis and control of grid connected DFIG and solar PV based hybrid energy system,” *Proc. 2016 Int. Renew. Sustain. Energy Conf. IRSEC 2016*, pp. 1104–1109, 2017.

[29] Y. Lei, A. Mullane, G. Lightbody, and R. Yacamini, “Modeling of the wind turbine with a doubly fed induction generator for grid integration studies,” *IEEE Trans. Energy Convers.*, vol. 21, no. 1, pp. 257–264, 2006.

[30] A. I. Said and B. Mandoko Na Mpeya, “Sub- and Super-Synchronous Induction Motor-Thyristor Cascade Control,” *IFAC Proc. Vol.*, vol. 16, no. 16, pp. 345–352, 1983.

[31] K. A.-H. Haitham Abu-Rub, Mariusz Malinowski, Ed., *Power Electronics for renewable Energy Systems, Transportation and Industrial Applications*, First. IEEE Press and John Wiley & Sons Ltd.

[32] A. Dendouga, R. Abdessemed, M. L. Bendaas, and A. Chaiba, “Decoupled active and reactive power control of a doubly-fed induction generator (DFIG),” *2007 Mediterr. Conf. Control Autom. MED*, no. 1, 2007.

[33] A. Petersson, “Analysis, modeling and control of doubly-fed induction generators for wind turbines,” *Doktorsavhandlingar vid Chalmers Tek. Hogsk.*, no. 2282, 2005.

[34] J. Lepka and P. Stekl, “3-Phase AC Induction Motor Vector Control Using a 56F80x, 56F8100 or 56F8300 Device,” *Control*, 2001.

[35] A. Report, “Sensorless Field Oriented Control of 3-Phase Induction Motors Using Control Law Accelerator (CLA),” no. October, pp. 1–44, 2013.

[36] A. I. Said and B. Mandoko Na Mpeya, “Sub- and Super-Synchronous Induction Motor-Thyristor Cascade Control,” *IFAC Proc. Vol.*, vol. 16, no. 16, pp. 345–352, 1983.

[37] K. A.-H. Haitham Abu-Rub, Mariusz Malinowski, Ed., *Power Electronics for renewable Energy Systems, Transportation and Industrial Applications*, First. IEEE Press and John Wiley & Sons Ltd.

[38] A. I. Said and B. Mandoko Na Mpeya, “Sub- and Super-Synchronous Induction Motor-Thyristor Cascade Control,” *IFAC Proc. Vol.*, vol. 16, no. 16, pp. 345–352, 1983.

[39] K. A.-H. Haitham Abu-Rub, Mariusz Malinowski, Ed., *Power Electronics for renewable Energy Systems, Transportation and Industrial Applications*, First. IEEE Press and John Wiley & Sons Ltd.

[40] A. Dendouga, R. Abdessemed, M. L. Bendaas, and A. Chaiba, “Decoupled active and reactive power control of a doubly-fed induction generator (DFIG),” *2007 Mediterr. Conf. Control Autom. MED*, no. 1, 2007.

[41] A. I. Said and B. Mandoko Na Mpeya, “Sub- and Super-Synchronous Induction Motor-Thyristor Cascade Control,” *IFAC Proc. Vol.*, vol. 16, no. 16, pp. 345–352, 1983.

[42] K. A.-H. Haitham Abu-Rub, Mariusz Malinowski, Ed., *Power Electronics for renewable Energy Systems, Transportation and Industrial Applications*, First. IEEE Press and John Wiley & Sons Ltd.

[43] A. Dendouga, R. Abdessemed, M. L. Bendaas, and A. Chaiba, “Decoupled active and reactive power control of a doubly-fed induction generator (DFIG),” *2007 Mediterr. Conf. Control Autom. MED*, no. 1, 2007.

[44] A. Petersson, “Analysis, modeling and control of doubly-fed induction generators for wind turbines,” *Doktorsavhandlingar vid Chalmers Tek. Hogsk.*, no. 2282, 2005.

[45] J. Lepka and P. Stekl, “3-Phase AC Induction Motor Vector Control Using a 56F80x, 56F8100 or 56F8300 Device,” *Control*, 2001.

[46] A. Report, “Sensorless Field Oriented Control of 3-Phase Induction Motors Using Control Law Accelerator (CLA),” no. October, pp. 1–44, 2013.

[47] A. Verma, A. Chakraborti, B. Das, P. R. Kasari, M. Mishra, and S. Pal, “A new topology for hybrid wind-solar generation system for isolated loads,” *Proc. 2018 IEEE Int. Conf. Power, Instrumentation, Control Comput. PICC 2018*, pp. 1–7, 2018.

[48] G. Abad, *Power Electronics and Electric Drives for Traction Applications*. 2016